Placental Hypoxia During Early Pregnancy Causes Maternal Hypertension and Placental Insufficiency in the Hypoxic Guinea Pig Model 1

Authors: Thompson, Loren P., Pence, Laramie, Pinkas, Gerald, Song, Hong, and Telugu, Bhanu P.

Placental Hypoxia During Early Pregnancy Causes Maternal Hypertension and Placental Insufficiency in the Hypoxic Guinea Pig Model[1]

Loren P. Thompson,[2,4,5,6] Laramie Pence,[4,7,8] Gerald Pinkas,[5,6] Hong Song,[5,6] and Bhanu P. Telugu[3,4,7,8]

[5]Department of Obstetrics, Gynecology and Reproductive Sciences, University of Maryland, Baltimore, Maryland
[6]University of Maryland School of Medicine, Baltimore, Maryland
[7]Animal Biosciences and Biotechnology Laboratory, USDA-ARS, Beltsville, Maryland
[8]Animal and Avian Science, University of Maryland, College Park, Maryland

ABSTRACT

Chronic placental hypoxia is one of the root causes of placental insufficiencies that result in pre-eclampsia and maternal hypertension. Chronic hypoxia causes disruption of trophoblast (TB) development, invasion into maternal decidua, and remodeling of maternal spiral arteries. The pregnant guinea pig shares several characteristics with humans such as hemomonochorial placenta, villous subplacenta, deep TB invasion, and remodeling of maternal arteries, and is an ideal animal model to study placental development. We hypothesized that chronic placental hypoxia of the pregnant guinea pig inhibits TB invasion and alters spiral artery remodeling. Time-mated pregnant guinea pigs were exposed to either normoxia (NMX) or three levels of hypoxia (HPX: 16%, 12%, or 10.5% O_2) from 20 day gestation until midterm (39–40 days) or term (60–65 days). At term, HPX (10.5% O_2) increased maternal arterial blood pressure (HPX 57.9 $\pm$ 2.3 vs. NMX 40.4 $\pm$ 2.3, $P < 0.001$), decreased fetal weight by 16.1% ($P < 0.05$), and increased both absolute and relative placenta weights by 10.1% and 31.8%, respectively ($P < 0.05$). At midterm, there was a significant increase in TB proliferation in HPX placentas as confirmed by increased PCNA and KRT7 staining and elevated *ESX1* (TB marker) gene expression ($P < 0.05$). Additionally, quantitative image analysis revealed decreased invasion of maternal blood vessels by TB cells. In summary, this animal model of placental HPX identifies several aspects of abnormal placental development, including increased TB proliferation and decreased migration and invasion of TBs into the spiral arteries, the consequences of which are associated with maternal hypertension and fetal growth restriction.

animal model, hypoxia, placental insufficiency, maternal hypertension, pregnancy

INTRODUCTION

An appropriate tissue oxygen (O_2) balance is important for normal placental development. Several conditions such as living at high altitude, maternal disease (cyanotic heart disease), anemia, infection, and chronic inflammation [1] can result in decreased blood and O_2 supply and placental insufficiency [2]. Abnormal placental function manifests as altered endocrine function and/or nutrient transport and can result in a range of maladies from small for gestational age babies to maternal conditions such as pre-eclampsia (PE). PE is one of the leading causes of maternal and infant illness and death [3] and often presents as hypertension, vascular inflammation, edema, and proteinuria [4] in the mother and asymmetric growth restriction in the fetus [5]. Even though placental hypoxia (HPX) is implicated in placental disorders and fetal growth restriction (FGR), the role of O_2 in placental development and trophoblast (TB) differentiation remains unclear. Understanding the molecular basis of HPX-induced placental dysfunction is key to identifying causal factors of placental insufficiencies, pregnancy-induced maternal hypertension, and FGR [6].

In human pregnancy, placental development is initiated at embryo implantation followed by a regulated set of events, including TB proliferation and migration into the decidua, and culminating in the invasion and remodeling of maternal spiral arteries [7]. During early stages of embryo implantation, TB proliferation and migration occur under low O_2 conditions in the maternal decidua [7]. This is followed by maternal spiral artery remodeling by invasive TBs and increased blood perfusion and oxygenation of the placenta [7, 8]. The role of O_2 in mediating TB differentiation and endovascular invasion is controversial because of conflicting in vitro results showing that low O_2 conditions promote TB proliferation and decrease invasion in cell culture [9–11], whereas others have shown that hypoxic conditions (1% O_2) increase cultured HRT-8/Svneo cell invasion through Matrigel [12, 13]. These conflicting results point to limitations of a simplistic in vitro system, lacking interactions with maternal decidual cells and complex microenvironment that exists in the animal model. Another plausible explanation is the differences in the starting TB cell types that could be at different stages of differentiation.

In humans, placental pathologies are typically initiated in the first trimester of pregnancy and not identified until the last trimester. While studies of term placenta permit investigation of the consequences of disease, they fail to provide the means for studying the pathogenesis of disease. Additionally, term placenta lacks a placental bed, thereby precluding investigation of the site of pathogenesis. These limitations necessitate investigation of placental diseases prior to term and preferably during the early stages of placentation. While the pregnant baboon is the best surrogate to the human for studying

placental development [14], the pregnant guinea pig makes for a less expensive and ideal alternative because of close similarities to the human placenta [14–17]. Similar to humans, the guinea pig has a hemomonochorial placenta and exhibits a characteristic deep invasion into the maternal decidua (a limitation in most rodent models) [7]. The guinea pig placenta consists of several lobules with a maternal arterial channel in the center surrounded by a single fetal syncytiotrophoblast layer. The labyrinthine lobes are distinct units of feto-maternal circulatory exchange embedded in maternally perfused inter-lobia that drain the labyrinth of maternal blood. A unique feature of the guinea pig placenta is the subplacenta, which is a highly folded derivative of TB shell consisting of a cellular TB layer that is analogous to the cell columns of the anchoring chorionic villi of human placenta [17]. The subplacenta harbors a proliferating population of TBs that invade into the maternal endometrium and can be traced in the interstitium, blood vessels, and myometrium. In addition to the placental organization, the pregnant guinea pig also mimics the human in having a maternal progesterone profile that does not decline at term [14] as well as fetal growth characteristics (i.e., growth, and fat/protein accretion rates) and relative maturity at the time of birth [14, 15, 18].

In the present study, a pregnant guinea pig model was used to investigate the placental response to sustained HPX and assess the impact of altered placental development on both maternal and fetal phenotypes in late gestation. We hypothesized that a chronic reduction in O_2 levels during placental development disrupts the transitional process of cytotrophoblasts from a proliferative to invasive subtype, thereby altering spiral artery remodeling and eventually giving rise to placental insufficiency and potential PE-like symptoms.

MATERIALS AND METHODS

Generation of the Hypoxic Animal Model

All animal procedures using guinea pigs were approved by the University of Maryland Institutional Animal Care and Use Committee in accordance with Association for Assessment and Accreditation of Laboratory Animal Care International-accredited procedures. Successful pregnancy was determined by palpation, which occurs as a solid lump of 1 cm in diameter at 20–23 days of gestation [19]. Pregnant guinea pigs were housed in either room air (normoxia [NMX], n = 10) or in a chamber containing either 16% (n = 4), 12% (n = 5), or 10.5% O_2 (n = 10) HPX at 28–30 days of gestation; each were maintained in their respective environments for the duration of pregnancy. In guinea pigs, the TB invasion into uteroplacental arteries of the placenta begins at ~3 wk gestation [19]. We have chosen the timing of exposure to maternal HPX a few days later to ensure a successful implantation but early enough to impact the invasive process. The level of HPX at 10.5% O_2 was selected based on the O_2 level to which high-altitude (3500–4500 m) populations at risk of PE and FGR are naturally exposed [20] and the minimal level to prevent termination of the guinea pig pregnancy. Additionally, as we have previously reported, exposure to 10.5% O_2 reduces maternal arterial O_2 saturation from 97.7% to 66.1% (NMX vs. HPX, respectively) [21], which causes fetal HPX as indicated by increased fetal cardiac HIF1 (hypoxia inducible factor-1) protein levels [22] and fetal liver hypoxyprobe staining [23]. Maternal food intake (g/day/maternal kg), water intake (ml/day/maternal kg), and maternal weight gain (g/day) were measured every 2 days over the last 14 days of pregnancy (50–64 days of gestation). Both NMX and HPX pregnant guinea pigs were terminated just prior to term (term = 65 days of gestation) with the identification of pelvic separation of 1 cm. A separate group of animals were exposed to 10.5% O_2 at 28–30 days of gestation, and placentas and fetuses were extracted at 40 days of gestation to assess HPX effects at midterm. In addition, nonpregnant female guinea pigs were exposed to either NMX (n = 8) or HPX (10.5% O_2, n = 8) for the same duration (35 days) as pregnant animals and served as controls.

Blood Pressure Measurement

Maternal arterial blood pressures of both NMX and HPX (16%, 12%, 10.5% O_2) pregnant guinea pigs were measured at term (n = 4–10; four groups) prior to fetal extraction. Blood pressure from nonpregnant female guinea pigs was measured similarly after 35 days exposure of 10.5% O_2 HPX or NMX exposure. Animals were anesthetized (ketamine, 80 mg/kg intraperitoneally [i.p.], and xylazine, 1 mg/kg i.p.), heparinized, and a cannula inserted into the right brachial artery for measurement of blood pressure. Systolic blood pressure (SBP), diastolic blood pressure (DBP), and mean arterial pressure (MAP) were recorded on a data acquisition system (ADInstruments) and analyzed using ADInstruments Chart version 4.2 software.

Tissue and Urine Extraction

Maternal (heart and kidney) and fetal organs (heart, brain, liver, and kidney) were extracted after terminal anesthesia from NMX and HPX pregnant animals at term. Absolute fetal organ weights were measured, and relative weights were normalized to their respective body weights (Supplemental Table S1; Supplemental Data are available online at www.biolreprod.org). Likewise, placentas were extracted from both NMX and HPX at 40 days and 65 days of gestation animals and weighed and stored at −80°C until used for gene expression analysis. Maternal urine was collected by syringe from the bladder at the time of fetal organ extraction from NMX (n = 6) and HPX (10.5% O_2, n = 6) guinea pigs (65 days of gestation; subset of animals used to measure blood pressures) and immediately frozen. Total protein was measured by the Bradford method normalized to creatinine levels (Cayman Chemicals).

Immunohistochemistry

To examine placental morphology of maternal blood vessels at midterm, NMX and HPX (10.5% O_2) animals (40 days of gestation, n = 3 each group) were perfusion fixed with 4% paraformaldehyde on the maternal side following cannulation of the uterine artery and drainage of the uterine vein. Fixed placentas were paraffin embedded via standard protocol. Immunohistochemistry was performed on 5 μm sections, subjected to heat-induced antigen retrieval at 95°C for 20 min in 10 mM Tris, 1 mM ethylenediamine-tetraacetic acid, pH 9.0, rinsed in TBST (20 mM Tris, 150 mM NaCl, and 0.1% Tween, pH 7.4), blocked using Dako Protein Block, and then incubated with primary antibodies (Cytokeratin 7/KRT7, PCNA, smooth muscle actin, von Willebrand factor; Supplemental Table S2) overnight at 4°C. On the next day, sections were washed in TBST and incubated with secondary antibodies (fluorophore- or enzyme-conjugated antibodies, i.e., alkaline phosphatase [AP] or horseradish peroxidase [HRP]), for 1 h at room temperature. For immunofluorescence, sections were incubated with the following secondary antibodies diluted in TBST—Alexa Fluor 488 goat anti-mouse IgG2a (1:500) and/or Alexa Fluor 568 goat anti-rabbit (1:500)—then slides were mounted with Prolong-Gold Antifade Mount with 4′,6-diamidino-2-phenylindole (DAPI) (Life Technologies), which stained the nuclei. For enzymatic immunohistochemistry, sections were incubated with the following secondary antibodies diluted in TBST: goat anti-mouse IgG2a conjugated to HRP (1:100) and goat anti-rabbit conjugated to AP (1:100). The VECTOR Blue Alkaline Phosphatase Substrate kit (Vector Laboratories) was used for colorimetric detection of AP secondary antibodies and the DAB-Plus Substrate kit (Invitrogen) was used for detection of HRP secondary antibodies following the manufacturers' instructions. Sections were then counterstained with Nuclear Fast Red (Sigma-Aldrich) to stain nuclei and then mounted with ImmunoHistomount medium (Abcam). In all experiments, negative controls were performed in which no primary antibody was used.

To demonstrate local placental HPX, the hypoxyprobe-1 (pimonidazole hydrochloride, Hypoxyprobe-1 Kit; Chemicon) was administered (80 mg/kg, i.p.) to a single NMX and HPX (10.5% O_2) pregnant guinea pig at 40 days of gestation for 90 min. Animals were anesthetized and placentas were extracted, fixed, and embedded for immunofluorescence staining of the reduced pimonidazole adducts for detection of placental HPX. Pimonidazole adducts, which form under conditions of tissue O_2 level <10 mmHg [24], were probed using hypoxyprobe-1 antibody (see Supplemental Methods for the full protocol).

Histological Measurements of Placenta

To capture images of the entire placenta, tissue sections of 5 μm were stained with hematoxylin and eosin (H&E) by standard procedures and multiple 1.8× images were captured and assembled into a single high-resolution image using Adobe Photoshop. Areas were measured manually using the freehand selection tool and the area calculation feature of ImageJ software (National Institutes of Health). To reduce variability and eliminate user bias, all measurements were taken three times each by two separate individuals. The areas were averaged for three placentas from each treatment group.

Quantitative RT-PCR of Placenta Tissues

Placentas of 40 days and 65 days of gestation of NMX and HPX (10.5% O_2) guinea pigs were used to measure mRNA levels of selected genes. Total RNA was isolated from snap-frozen tissues using TRIzol (Life Technologies) in combination with RNeasy Mini Kit (Qiagen) reagents, and DNA removed using the TURBO DNA-free kit (Ambion). Two micrograms of total RNA was reverse transcribed using Superscript III First-Strand Synthesis System (Invitrogen) with random hexamer primers following the manufacturer's protocol. Quantitative real-time PCR was performed using SYBR Green PCR Master Mix (Life Technologies) on an Applied Biosystems 7500 Real-Time PCR system using gene-specific primers (Supplemental Table S3). The comparative ΔCT method [25] was used to analyze gene expression changes between the treatment groups. There were five to six biological replicates and two technical PCR replicates for each placental sample of the four treatment groups that include NMX (n = 5) and HPX (10.5% O_2, n = 6) at 40 days of gestation and NMX (n = 5) and HPX (10.5% O_2, n = 5) at 65 days of gestation.

Statistical Analysis

Data are expressed as mean ± SEM. Comparisons between groups were made using a one-way ANOVA on Ranks with HPX treatment as the independent variable. If mean values among multiple comparisons were found to be different ($P < 0.05$), a Dunn post hoc test for unequal sample numbers was applied to analyze differences from NMX controls. For comparisons of fetal body weight and placenta weight, all fetuses and placentas from litters of the four treatment groups were included for comparison. For histology and gene expression analysis, separate placentas from the same litter were selected for analysis as representative of the litter and represents n = 1. Statistical comparisons for MAP and fetal and placenta weights were performed with SigmaStat software, and comparisons for real-time PCR data was analyzed by unpaired t-test using Prism 7 software using the PROC generalized linear model method.

RESULTS

Effects of HPX on Maternal Parameters

Arterial blood pressures from pregnant and nonpregnant animals were measured in guinea pigs exposed to NMX or three different levels of HPX conditions (Fig. 1A). In pregnant animals, the MAP, SBP, and DBP were significantly elevated ($P < 0.05$) at 10.5% O_2 HPX compared to NMX controls (MAP: 57.9 ± 2.3 vs. 40.4 ± 2.3; SBP: 65 ± 2.8 vs. 47.0 ± 2.4; DBP: 50.6 ± 1.9 vs. 34.5 ± 2.1 mmHg for HPX at 10.5% O_2 vs. NMX, respectively) (Fig. 1A and Supplemental Fig. S1). However, the MAP in pregnant animals exposed to 12% or 16% O_2 HPX conditions was not significantly elevated. Likewise, 10.5% O_2 HPX did not result in elevated MAP (50.9 ± 2.6 mmHg vs. 47.6 ± 2.6 mmHg, HPX vs. NMX, respectively) in nonpregnant animals.

Histological analysis of maternal kidneys revealed no pathogenesis in glomeruli of HPX compared to NMX animals, respectively (Supplemental Fig. S2). Furthermore, there was no significant difference in urine protein/creatinine ratios (n = 6 each group; 0.184 ± 0.034 vs. 0.212 ± 0.044 mg protein/mg creatinine). The average food intake (50.8 ± 3.9 vs. 49.5 ± 4.0 g/day/kg, NMX vs. HPX, respectively), water intake (208.7 ± 33.0 vs. 231.0 ± 36.8 ml/day/kg, NMX vs. HPX, respectively), and the maternal weight gain (12.6 ± 2.3 vs. 15.9 ± 6.5 g/day, NMX vs. HPX, respectively) were not significantly different between NMX and HPX animals (10.5% O_2).

Effects of HPX on Fetal Parameters

Maternal exposure to 10.5% O_2 HPX (but not 12% or 16% O_2) resulted in reduced fetal weight ($P < 0.05$) by 16.1% relative to NMX controls (Fig. 1B and Supplemental Table S1), but increased ($P < 0.05$) both absolute and relative placental weights by 10.1% and 31.8%, respectively (Fig. 1, C and D,

and Supplemental Table S1). However, reduction of fetal weights or increase in absolute or relative placental weights was not observed at 12% or 16% O_2 (Fig. 1, C and D, and Supplemental Table S1) conditions. Hypoxyprobe analysis confirmed that exposure to maternal HPX (10.5% O_2) at 40 days of gestation induced a local tissue HPX in the guinea pig placenta, which was absent in the NMX control (Fig. 1E). The average litter size per pregnant guinea pig range from three to four pups/litter (3.7 ± 0.2 for NMX, 3.0 ± 0.6 for HPX 16% O_2, 3.2 ± 0.4 for HPX 12% O_2, and 3.5 ± 0.2 for HPX 10.5% O_2).

Exposure to HPX had variable and asymmetric effects on fetal organ (brain, heart, liver, and kidney) weights. Chronic 10.5% O_2 HPX resulted in reduced ($P < 0.05$) fetal brain and liver weights (Supplemental Table S1). However, the relative weights (ratio of weight of organs to fetal weight) of fetal liver was decreased, while fetal brain and heart were increased ($P < 0.05$) with HPX (10.5% O_2). The absolute or relative weights of kidney remained unaffected in all HPX treatments. At relatively mild HPX conditions, specifically 16% and 12% O_2, only the absolute fetal brain weight showed significant reduction at 12% O_2 conditions ($P < 0.05$; Supplemental Table S1).

Effects of HPX on Morphology of Midterm (40 Days) Placentas

The NMX and HPX (10.5% O_2) placentas harvested at 40 days of gestation were examined for subplacenta and labyrinth morphology as well as TB invasion in the junctional zone. Subplacenta is a villous-like structure (Fig. 2) and a source of invasive TBs in the guinea pig placenta prominent at 40 days of gestation, but disappears at term [26]. Immunofluorescence staining of smooth muscle actin (SMA) (green; Fig. 2A), which stains for maternal blood vessels and decidual cells, in NMX (top row) and HPX (bottom row) placentas revealed a noticeable expansion of the junctional zone in the maternal decidua of 10.5% O_2 HPX animals. On the maternal side, HPX placentas underwent an exaggerated decidual response that led to an expansion of the junctional zone (Fig. 2, A and B, and Supplemental Fig. S3). Both low (Fig. 2A) and high (Fig. 2B) magnification images show a net proliferation of decidual cells containing eosinophilic cytoplasm lining the myometrium (Supplemental Fig. S3) in the HPX (seen as a clear and broad boundary in the junctional zone) compared to NMX placenta.

In the subplacenta region, costaining of mononucleated KRT7-positive TBs (blue) and SMA (brown; Fig. 3A) revealed a noticeable narrowing of blood spaces in HPX placentas. As shown in Figure 3B, there was a trend toward increase in subplacenta area as a fraction of total placental area (placenta plus labyrinth; Fig. 3B) in HPX placenta. The narrowing of blood spaces and increase in subplacenta area is a consequence of significantly increased ($P < 0.05$) proliferation of KRT7-positive mononuclear TB cells as evidenced by proliferative marker PCNA staining (Fig 3, C and D). Staining of both KRT7-positive TBs (red, middle panel; Fig. 3C) and proliferating cell marker PCNA (green, right panel; Fig. 3C) were increased in the subplacenta of HPX placentas (Fig. 3D). In the labyrinthine area, HPX caused an expansion of blood channels as indicated by increased diameters of maternal arterial channels (Fig. 3, E and F).

One of the cardinal functions of invasive TBs is the remodeling of maternal arteries. In 40 day NMX placenta, KRT7-positive cells were identified within the blood vessels lining the lumen in both proximal and distal maternal arteries (Fig. 4 and Supplemental Figs. S4 and S5). In the HPX
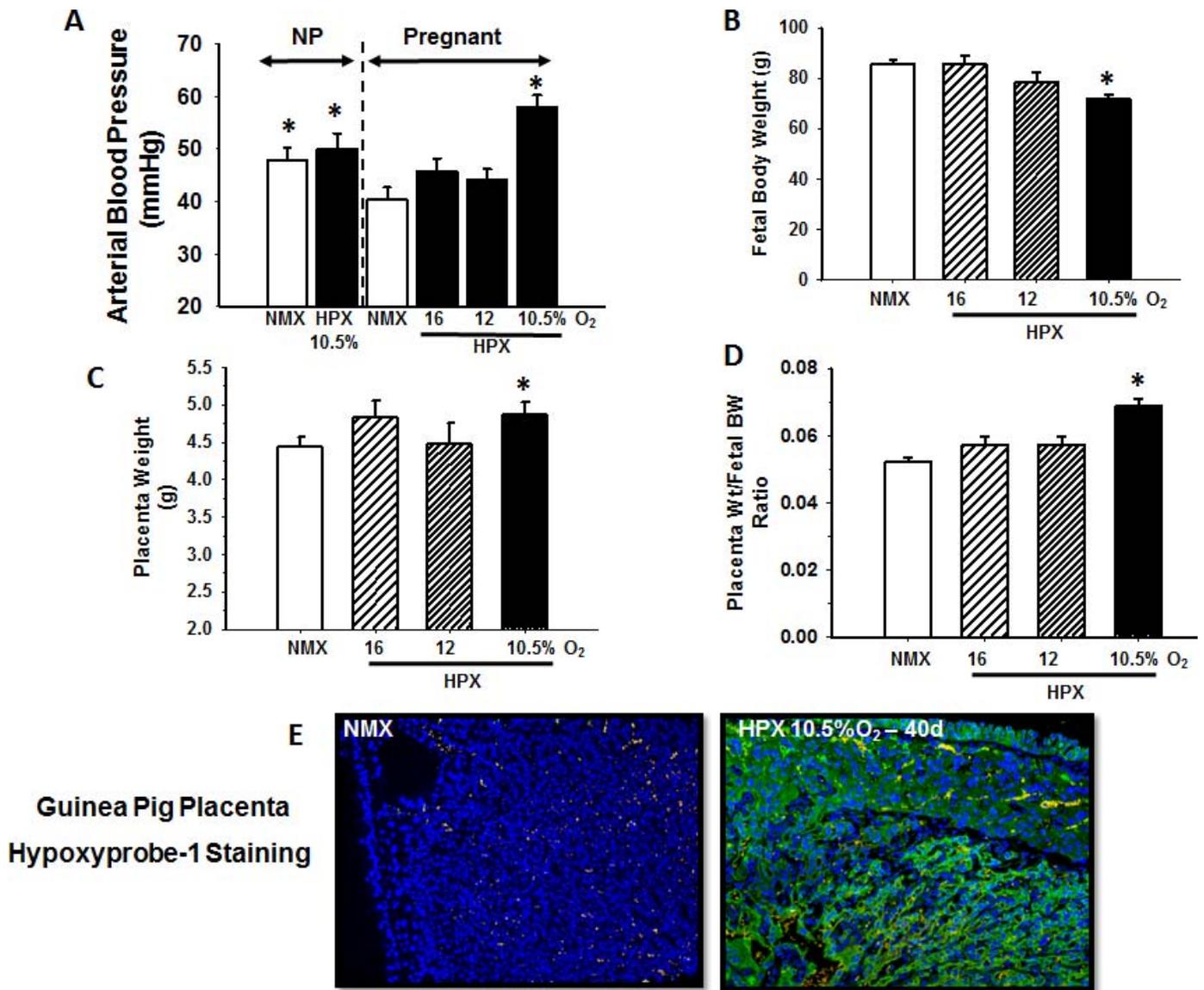
FIG. 1. Effects of systemic hypoxia (HPX) on guinea pig dam, placenta, and fetus. A) Effects of HPX on mean arterial blood pressures (MAP) of nonpregnant and pregnant (term = 65d gestation) guinea pigs. The MAP values of nonpregnant female guinea pigs (NMX, open bar, n = 8; HPX, closed bar, n = 10) and HPX (16%, n = 4; 12%, n = 5; 10.5%, n = 10) on the right. In the figure, the asterisk (*) indicates P < 0.05 versus NMX pregnant. Absolute fetal (B) and placenta weights (g) (C) and relative placenta weights (placenta weight/fetal body weight ratios) (D) are shown for normoxic (NMX, open bar, n = 36) and hypoxic (HPX, hashed bars, 16%, n = 12; 12%, n = 15; and 10.5% O₂ n = 38) animals. Values were obtained from all fetuses of litters from pregnant animals. In the figure, the asterisk (*) indicates P < 0.05 versus NMX controls. E) Immunofluorescence staining of hypoxyprobe-1 (pimonidazole-fluorescent, green) and DAPI (blue nuclear stain) of NMX and HPX (10.5% O₂) placenta at 40 days of gestation. The HPX placenta (200×) exhibits fluorescent staining in cytotrophoblasts throughout the labyrinth, whereas the NMX placenta showed no fluorescent staining in any of the sections viewed. Red blood cells are identified as orange fluorescence within the lumen of blood vessels. Mouse serum was used as a negative control, which showed no fluorescent stain (not shown).

placenta, there was little to no KRT7-positive cells located within maternal blood vessels. Even though some KRT7-positive cells were seen in vessels closer to the subplacenta, no KRT7 staining was seen in the walls of vessels located close to the myometrium and distal arteries, nor was there any evidence of widening of the lumen in the HPX placenta. Instead, there was an increased abundance of SMA-positive decidual stromal cells lining the blood vessels and fewer KRT7-positive cytotrophoblast cells (Fig.4 and Supplemental Figs. S4 and S5). Quantitative image analysis of multiple samples (derived from Fig. 4 and Supplemental Fig. S4; NMX and HPX, n = 3) showed a decrease in the ratio of KRT7 to von Willebrand factor signal (normalized to SMA; Supplemental Fig. S6) in the

junctional zone of HPX placenta, indicating that HPX has an inhibitory effect on the ability of extravillous TBs to invade and remodel the endothelial lining of the maternal spiral arteries in the junctional zone.

Effects of HPX on Placental Gene Expression

We examined the effect of chronic maternal HPX (10.5% O₂) on placenta gene expression at 40 days (midterm) and 65 days of (term) gestation relative to NMX controls (Fig. 5, A and B). Midterm and term placentas were exposed to HPX for 15 and 40 days duration, respectively. This provided a means for assessing how placental gene expression differs with duration of HPX relative to its age-matched NMX control. A
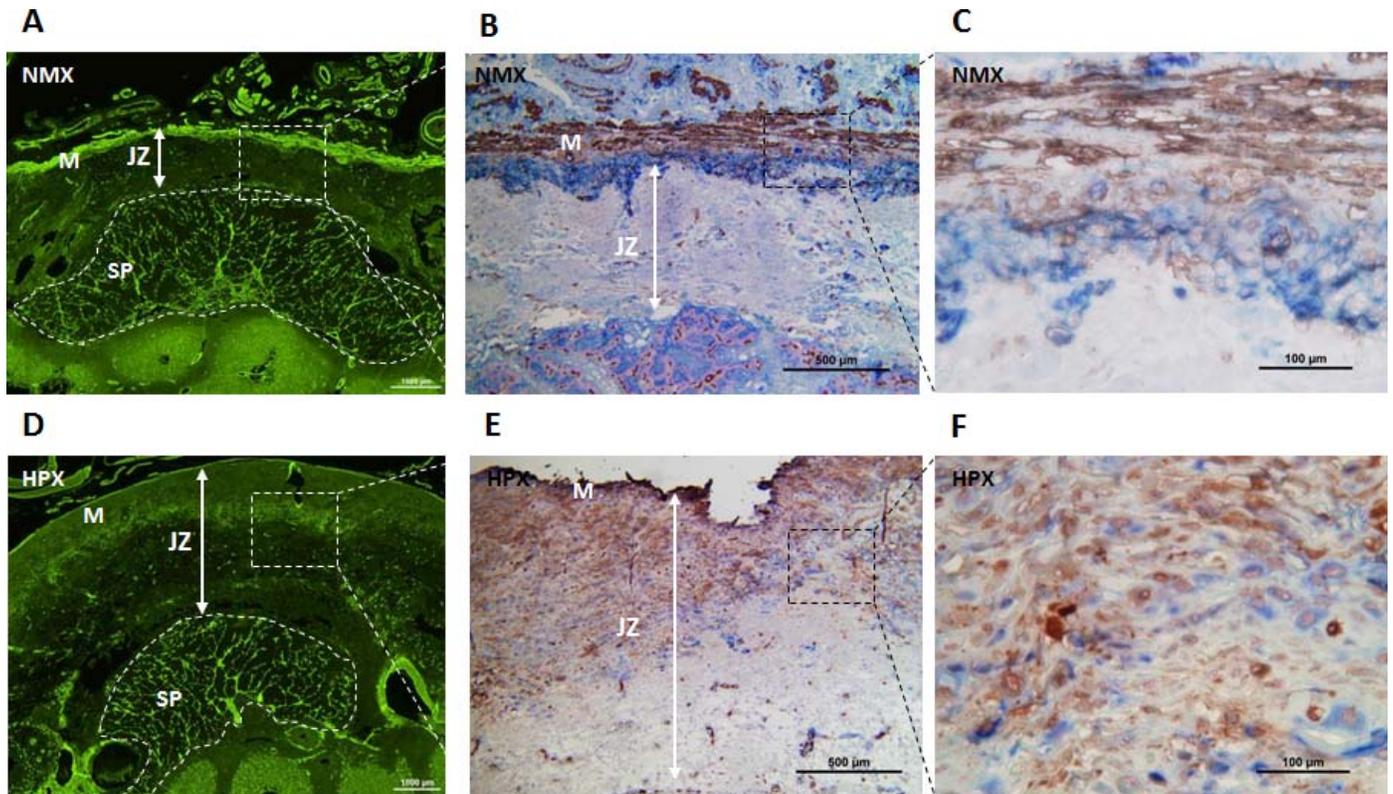
FIG. 2. Effects of hypoxia (HPX) on junctional zone (JZ) and decidua of normoxic (NMX) and hypoxic (HPX, 10.5% O_2) guinea pig placentas at 40 days of gestation (term = 65 days of gestation). In **A** and **D**, immunofluorescence staining of NMX and HPX placentas is identified for smooth muscle actin (SMA), which stains for blood vessels and decidual cells across sections of the myometrium (M), maternal decidua, JZ, and subplacenta (SP). In HPX placentas, an increased decidual cell layer in the JZ was noticed compared to the NMX placenta. Panels (**B**, **C** [NMX] and **E**, **F** [HPX]) show low (**B**, **E**) and high (**C**, **F**) magnification images with costaining for decidual stromal cells, SMA (brown), and KRT7-positive TB cells (blue). Notice an expanded SMA-positive stromal cell population indicative of an increased decidualization response in HPX animals (**E**, **F**). Bars = 1000 μm (**A**, **D**), 500 μm (**B**, **E**), and 100 μm (**C**, **F**).

1.4-fold change was considered a cutoff level for up- or downregulation (dotted line) and a $P < 0.05$ (*) and $P < 0.01$ (**) was considered statistically significant (Fig. 5, A and B).

At midterm, HPX increased expression of the placental specific transcript, *ESX1*, and placental growth factor (*PGF*) while expression of syncytin (*ERVW1*), a syncytiotrophoblast marker and the main TB subtype in the labyrinth, was decreased (Fig. 5A). This is consistent with increased proliferation and decreased differentiation noticed in the subplacenta and labyrinth zones with HPX (Fig. 3) at midgestation. Expression of *HAND1*, a giant TB cell marker, was not significantly altered by HPX at either midterm or near-term gestation. Markers characteristic of PE and diseased placenta such as *FLT* and *PAPPA* were significantly increased in HPX, whereas *PTGS2*, a prostaglandin synthase marker, was decreased. Other markers such as vascular endothelial growth factor (*VEGF*), catechol O-methyl transferase (*COMT*), and tissue factor (*TF*, a coagulation factor) were not significantly different from control although showed a trend toward a decreased expression.

At term (65 days of gestation), HPX (10.5% O_2) placentas exhibited increased mRNA levels for *VEGF, PGF,* and *ESX1* compared to NMX controls accounting for compensatory increase in absolute or relative placental weights at term (Fig. 5, A and B). Expression of *HAND1* was upregulated while *ERVW1* expression was unaffected. Chronic HPX resulted in decreased expression levels of *PAPPA, PTGS2,* and *COMT*, increased levels of coagulation factor (TF), and had no effect on *FLT* levels. Thus, prolonged exposure to HPX induced compensatory changes in placenta gene expression, as indicated by increased *VEGF* and *PGF* and decreased *PAPPA, PTGS2,* and *COMT*.

DISCUSSION

The guinea pig has a hemomonochorial and labyrinthine placentation, and is composed of separate lobes each with independent circulation [27]. A distinguishing feature of guinea pig placenta is a highly folded and villous TB shell called the subplacenta. The subplacenta is analogous to the anchoring villi of the human placenta and is a source of invasive TB cells [27, 28]. During normal placenta development, local tissue HPX in the maternal decidua stimulates rapid TB proliferation and passive migration of TB from the subplacenta. As vasculogenesis progresses, there is increased tissue O_2 tension and a phenotypic switch of TBs from a proliferative to an invasive subtype [29], which culminates in an invasion of maternal spiral arteries and vascular remodeling [30]. In the present study, maternal HPX generated a sustained placental HPX and prevented vessel development and spiral artery remodeling. The placental response to the O_2 deprivation is an increased TB proliferation and subplacenta area, expanded decidua and junctional zone, nonremodeled maternal spiral arteries in the junctional zone, a compensatory increase in the volume of blood spaces in the labyrinth, and an increase in the overall weight of the placenta.

Chronic 10.5% O_2 HPX increased SBP, DBP, and MAP in pregnant animals but had no effect on blood pressures in
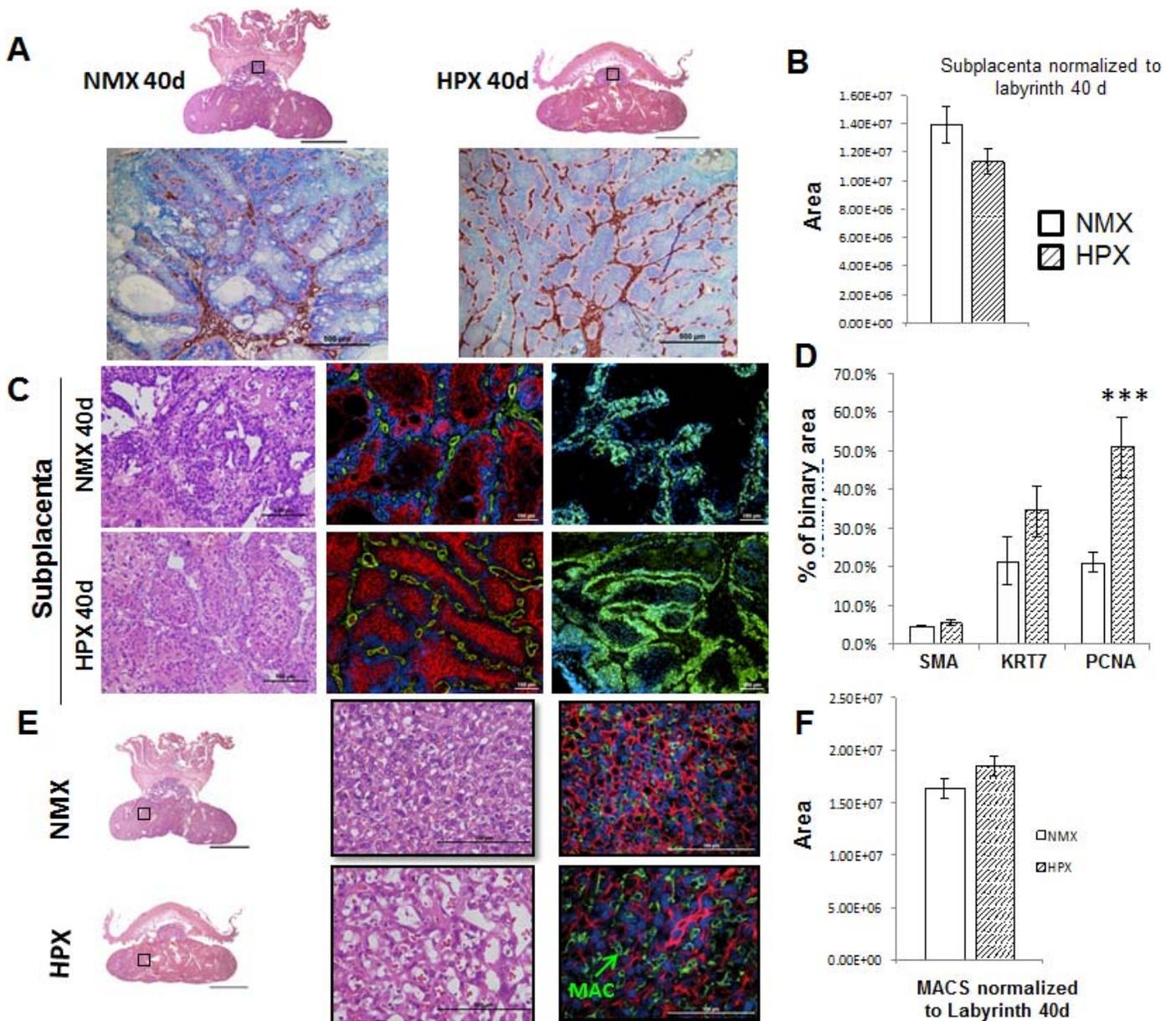
FIG. 3. Histological and immunohistochemical evaluation of normoxic (NMX) and hypoxic (HPX, 10.5% O$_2$) placentas (subplacenta, **A–D**; and labyrinth, **E–F**) at 40 days of gestation. **A**) Representative H&E whole images of NMX and HPX placentas shown at the top of the figure. In the panels below images (**A**), costaining of KRT7-positive TBs (blue), smooth muscle actin (SMA, brown), and nuclei (pink) shows increased proliferation of TBs and narrowed blood vessels in the subplacenta of HPX guinea pigs. **B**) Morphometric analysis of subplacenta area normalized to labyrinth area (percent of binary area) for NMX (black bar, n = 3) and HPX (grey bar, n = 3) placenta. **C**) In the subplacenta, staining by H&E (left panels) and immunofluorescence is used to identify KRT7-positive TBs (red), SMA (green), DAPI (nuclei, blue, middle panels), and proliferation in cytotrophoblasts (PCNA, green, right panels). **D**) Quantitative image analysis shows an increase of both KRT7 (TBs) and PCNA (proliferation) (*$P < 0.05$) staining in subplacenta of HPX (black bars) compared to NMX (grey bars) placentas. **E**) Effect of HPX on labyrinth morphology in NMX and HPX placentas. Representative whole images of NMX and HPX placentas (left), H&E (middle), and fluorescent staining (right) of KRT7-positive TBs (red), SMA (green), and DAPI/nuclei (blue) show an expansion of blood spaces in HPX placenta. **F**) Morphometric analysis of maternal arterial channels (MACs) in HPX (black bars) compared to NMX (grey bars) normalized to the labyrinth area is shown.

nonpregnant animals. The impact of maternal HPX on blood pressure is related to the severity of the HPX challenge because levels were not significantly elevated until 10.5% O$_2$ HPX. This is attributed to the presence of a hypoxic placenta, which was confirmed by hypoxyprobe staining, and no increase in blood pressures in nonpregnant guinea pig as a consequence of HPX. Consistent with the results in this study, HPX has been reported to inhibit uterine artery remodeling and reduce vasodilator reactivity to the flow of isolated arteries from pregnant guinea pigs exposed to high altitude but had no effect on arteries from nonpregnant guinea pigs [31, 32]. Several mechanisms may account for the HPX-induced increase in blood pressure, which include an increase in uteroplacental vascular resistance as a result of poor vascular remodeling and/ or release of vasoactive factors from the placenta into the maternal circulation [33], or both. In PE, release of vasoconstrictor factors such as soluble FLT1, angiotensin II, norepinephrine, and others from the placenta into the maternal circulation has been well established [6, 34]. However, the guinea pig model does not mimic PE-like symptoms as evident
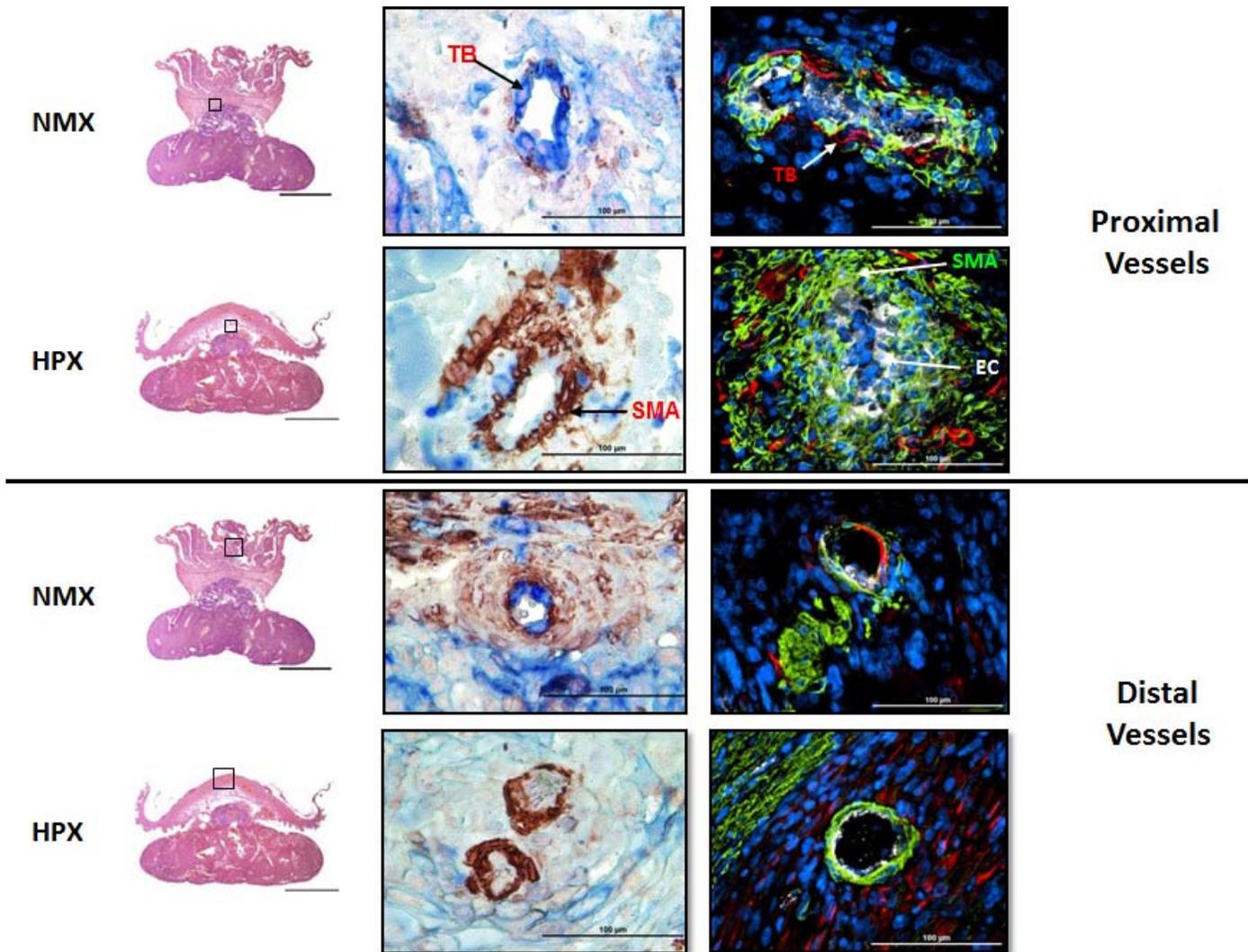
FIG. 4. Effects of HPX on endovascular invasion by trophoblasts (TBs) of proximal (top panels) and distal (bottom panels) vessels in normoxic (NMX) and hypoxic (HPX, 10.5% O_2) placentas at 40 days of gestation (term = 65 days of gestation). TBs and smooth muscle actin (SMA) are identified (middle panels) by KRT7-positive (blue) and brown colorimetric staining, respectively. The TB (KRT7 positive, red), SMA (green), and endothelial cells (EC, von Willebrand factor, white) were identified by immunofluorescent stain (right panels). There was a clear absence of both colorometric blue (KRT7 positive) and immunofluourescence red (KRT7 positive) in all sections viewed.

from the lack of renal dysfunction and glomerular endotheliosis [6, 34]. Further, it remains unclear whether HPX placentas release vasoconstrictor substances to account for the maternal hypertension in the current study. Regardless, it is plausible that both mechanisms of reduced placental perfusion and uteroplacental vessel remodeling [35] could contribute to increased maternal blood pressures in HPX animals. Evidence from this study points to poor vascular remodeling as a likely contributing factor for elevated arterial blood pressure. However, the release of vasoconstrictor factors produced from the HPX placenta [6] along with shearing of the spiral arterial endothelial lining could release membrane components into the maternal circulation [20], which has not been investigated in this study, contributing to elevated systemic vascular resistance and blood pressure.

At term, the HPX guinea pig placenta has undergone compensatory growth during the course of gestation. The increase in both absolute and relative placental weights indicates an adaptive response to the reduced oxygenation. This can be attributed to an HPX-induced increase in placenta tissue volume [36] and an increase in both blood spaces and vessel diameters in the labyrinth. Others reported increased [37, 38], decreased [39], and no change [36, 40] in placental weight with HPX, identifying differences in hypoxic severity, timing of gestation, and animal species. Despite the increased placental weight, fetal body weight is decreased compared to their NMX controls, clearly indicating an inefficient placenta. The HPX fetal guinea pigs exhibited asymmetric growth with heart and brain sparing, reduced relative liver weights, and no change in relative kidney weights. The growth response of HPX fetal guinea pigs is consistent with human studies that have measured growth restricted babies born from pregnant women living at high altitude [41–43]. Although hypophagia can accompany exposure to HPX depending on severity, this was not a factor in the current study because there was neither a reduction in maternal weight gain, food intake, nor water intake with maternal HPX (10.5% O_2). However, despite the presumably unaltered caloric intake, HPX may decrease fetal body weight by inducing metabolic changes [34] in the placenta that contribute to disruption of normal nutrient transport such as glucose to the fetus [44].
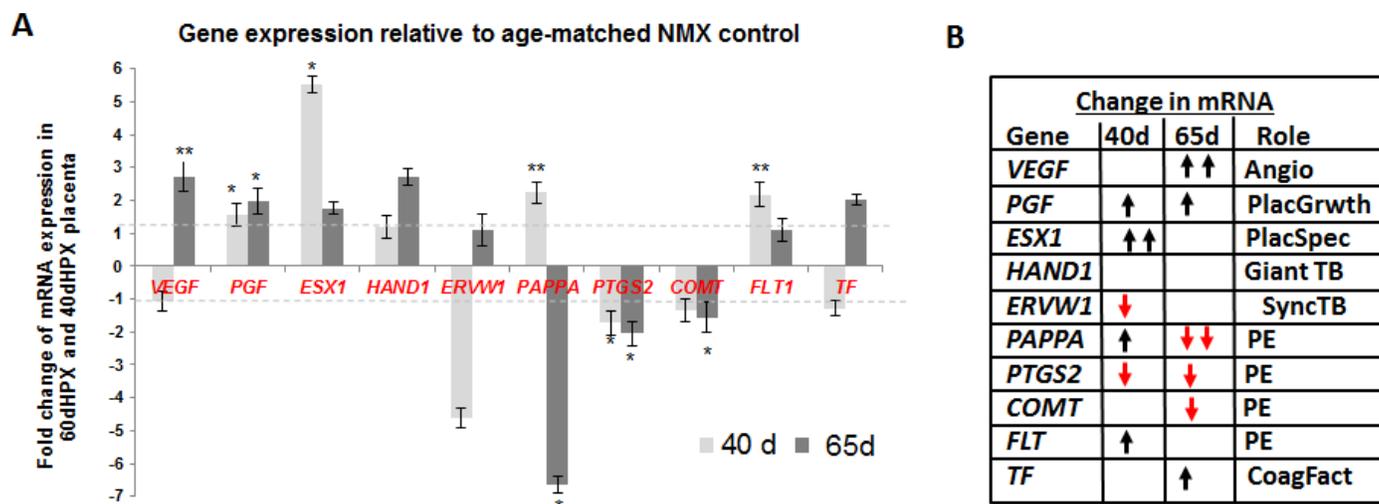
FIG. 5. Effects of hypoxia (HPX, 10.5% O_2; n = 6, 40 days; n = 6, 65 days) on placental mRNA expression relative to age-matched normoxic (NMX, n = 5 for each gestational age) controls. **A)** Fold changes of placental specific gene expression caused by HPX compared to age match NMX controls at midterm (40 days, light gray bars) and term (65 days, dark gray bars) pregnancy are shown. Data are normalized to endogenous beta-actin and expressed relative to NMX. Dashed line indicates 1.4-fold change, single or double asterisk denotes statistical difference $P < 0.05$ or $P < 0.01$ from NMX control, respectively. **B)** Table illustrates the directional changes (arrows) obtained from the gene expression data on the left along with identification of the role of each gene.

The morphological changes identified in HPX placenta at 40 days of gestation include an expanded junctional zone, increased TB proliferation, decreased subplacenta area, and reduced invasion of maternal arteries by TB. The expansion of the junctional zone was associated with a HPX-induced decidualization of the maternal endometrium. Despite an increase in TB proliferation in the maternal endometrium, there was a marked reduction in invasion of both proximal and distal maternal arteries by TBs. Furthermore, the reduction in vessel diameters within the subplacenta is suggestive of morphologic changes that could limit placental perfusion and generate a progressive decrease in tissue oxygenation over the course of gestation. The enhanced TB proliferation and increased vessel diameter in the labyrinth appears to be a compensatory response to HPX. In other studies, maternal HPX also expanded the labyrinthine zone in rats exposed to 12%–13% O_2 in late pregnancy [40, 45, 46] but was reduced if O_2 levels were lowered to 10% O_2 [46], indicating a threshold of HPX that may be maladaptive. HPX at 12%–13% O_2 in guinea pigs [36, 47] and mice [37, 46] increases the exchange surface area and maternal fetal diffusion capacity as an additional adaptive response. Thus, there are likely both adaptive and maladaptive competing influences that limit placental perfusion on the maternal side, while enhancing the capacity of nutrient transport in the labyrinth. This response is linked to the severity of the HPX and may manifest as FGR.

Maternal and fetal consequences of abnormal placental development such as in PE and placenta insufficiency are attributed to reduced spiral artery remodeling by mechanisms that are incompletely understood. The current animal model of the HPX pregnant guinea pig provides evidence that placental HPX stimulates TB proliferation in the maternal decidua but inhibits their invasion into both the proximal and distal arteries. This indicates a role for in vivo O_2 regulation in the switch of TBs to an invasive phenotype in the 40 day guinea pig placenta and is supported by 1) the presence of tissue HPX in the placenta, 2) increased TB proliferation in the maternal decidua and labyrinthine zone, and 3) marked reduction in TB invasion of the lumen of maternal arteries. Our data illustrate several examples where there was complete absence of TB invasion in HPX placentas in contrast to the presence of TB invasion in

NMX placentas. It is unclear if reduced TB invasion is associated with mechanisms that prevent invasion into the vessel wall under HPX conditions [48] or whether HPX stress inhibits TB differentiation [49, 50]. In vitro studies have shown that TBs remain in a proliferative phenotype under low O_2 conditions and differentiation into an invasive phenotype is prevented in HPX conditions [9, 51]. Furthermore, HPX (10.5% O_2 in vitro) has been shown to alter normal TB stem cell differentiation by inhibiting mitochondrial activity [50]. In contrast, pregnant rats exposed to 11% O_2 HPX between 6.5–13.5 days of gestation (term = 21 days of gestation) exhibited increased endovascular invasion of uterine mesometrial arteries by HIF-induced signaling of TB differentiation into an invasive subtype [52, 53]. The explanation for these contrasting results is unclear. This may reflect differences in the TB characteristics between the guinea pig and the rat because guinea pig TBs are more closely aligned with TBs of human placentas [18]. In addition, this may reflect differences in timing of gestational HPX stimulus at critical times of TB proliferation and/or differentiation within the placenta. Regardless, the HPX guinea pig model provides a means of using TB invasion as a distinct endpoint of spiral artery remodeling as the effects of maternal O_2 deprivation and placental HPX on uterine vascular resistance and fetal growth are investigated.

Gene expression of NMX and HPX placenta was measured to identify placental specific changes related to HPX and determine temporal changes that potentially contribute to adaptive responses of the placenta during the course of gestation. There were clear differences in gene expression in response to HPX at 40 days versus 65 days of gestation. At 40 days of gestation, both *PGF* and *ESX1* expression was increased and likely spurred the placental growth measured at term. At term, the increased expression of *VEGF* appears to be adaptive in promoting vasculogenesis as indicated by the increased blood spaces measured in the labyrinthine zone of HPX placentas. Expression of *PAPPA* is variable, exhibiting an increase in HPX placentas at 40 days of gestation followed by a significant decrease in expression at term. Its role in reducing insulin growth factor availability to the developing fetus may contribute to the FGR measured at term. The decrease in expression of syncytin (*ERVW1*) in midterm HPX placentas is

8

supportive of increased TB proliferation and decreased differentiation or commitment to syncytiotrophoblast population. There was a consistent decrease in several placental specific genes such as *PTGS2* and *COMT,* which generates 2-methoxyestradiol. Ablation of *COMT* and decline in 2-methoxyestradiol results in PE-like symptoms in mice, and a decline in *COMT* expression is observed in term HPX placenta. Elevated sFLT1 causes vascular injury and PE in humans. While sFLT1 is not annotated in guinea pigs, *FLT1,* a closest ortholog, showed a trend for upregulation with HPX, although not statistically significant at term. However, there was an upregulation of coagulation factor (TF) in HPX placenta at term, and we identified the formation of fibrin deposits in two out of three HPX placentas (Supplemental Fig. S7). An abundance of fibrin deposits in HPX placentas has been attributed to poorly perfused and PE placentas [43] caused by procoagulant activity of antigens released by apoptotic TB cells [43], which may also be contributing factors in our model (Supplemental Fig. S8). It should be noted that the composition of the placenta at midterm and term pregnant guinea pigs have clearly distinct compositions (e.g., loss of subplacenta at term). Furthermore, site-specific gene expression within placental regions (i.e., within the labyrinth as well as between the labyrinthine and junctional zones) may be an important consideration in matching temporal changes in placental morphology with exposure to chronic HPX.

In summary, this study indicates that placental HPX induces a compensatory blood vessel expansion in the guinea pig labyrinth in response to inhibited upstream arterial remodeling that generates maternal hypertension and FGR. Despite changes in maternal, placental, and fetal compartments, similar to that observed under conditions of PE, maternal renal function and morphology are unaffected, and likely reflects a placental insufficiency rather than PE-like symptoms. Thus, placental HPX of the guinea pig negatively impacts endovascular invasion by TBs, which may be an underlying cause of the maternal hypertension and FGR. Further study is needed to understand the temporal changes in decreased placental vessel remodeling as it relates to the compensatory response of the placenta.

REFERENCES

1. Hutter D, Kingdom J, Jaeggi E. Causes and mechanisms of intrauterine hypoxia and its impact on the fetal cardiovascular system: a review. Int J Pediatr 2010; 2010:401323.
2. Herrera EA, Riquelme RA, Ebensperger G, Reyes RV, Ulloa CE, Cabello G, Krause BJ, Parer JT, Giussani DA, Llanos AJ. Long-term exposure to high-altitude chronic hypoxia during gestation induces neonatal pulmonary hypertension at sea level. Am J Physiol Regul Integr Comp Physiol 2010; 299:R1676–R1684.
3. Ilekis JV, Reddy UM, Roberts JM. Preeclampsia–a pressing problem: an executive summary of a National Institute of Child Health and Human Development workshop. Reprod Sci 2007; 14:508–523.
4. Pennington KA, Schlitt JM, Jackson DL, Schulz LC, Schust DJ. Preeclampsia: multiple approaches for a multifactorial disease. Dis Model Mech 2012; 5:9–18.
5. Nardozza LM, Araujo Júnior E, Barbosa MM, Caetano AC, Lee DJ, Moron AF. Fetal growth restriction: current knowledge to the general Obs/Gyn. Arch Gynecol Obstet 2012; 286:1–13.
6. Redman CW, Sargent IL, Staff ACIFPA. Senior Award Lecture: making sense of pre-eclampsia–two placental causes of preeclampsia? Placenta 2014; 35(Suppl):S20–S25.
7. Kaufmann P, Black S, Huppertz B. Endovascular trophoblast invasion: implications for the pathogenesis of intrauterine growth retardation and preeclampsia. Biol Reprod 2003; 69:1–7.
8. Pringle KG, Kind KL, Sferruzzi-Perri AN, Thompson JG, Roberts CT. Beyond oxygen: complex regulation and activity of hypoxia inducible factors in pregnancy. Hum Reprod Update 2010; 16:415–431.
9. Genbacev O, Zhou Y, Ludlow JW, Fisher SJ. Regulation of human placental development by oxygen tension. Science 1997; 277:1669–1672.
10. Genbacev O, Joslin R, Damsky CH, Polliotti BM, Fisher SJ. Hypoxia alters early gestation human cytotrophoblast differentiation/invasion in vitro and models the placental defects that occur in preeclampsia. J Clin Invest 1996; 97:540–550.
11. Caniggia I, Mostachfi H, Winter J, Gassmann M, Lye SJ, Kuliszewski M, Post M. Hypoxia-inducible factor-1 mediates the biological effects of oxygen on human trophoblast differentiation through TGFbeta(3). J Clin Invest 2000; 105:577–587.
12. Graham CH, Postovit LM, Park H, Canning MT, Fitzpatrick TE. Adriana and Luisa Castellucci award lecture 1999: role of oxygen in the regulation of trophoblast gene expression and invasion. Placenta 2000; 21:443–450.
13. Graham CH, Lala PK. Mechanisms of placental invasion of the uterus and their control. Biochem Cell Biol 1992; 70:867–874.
14. Mitchell BF, Taggart MJ. Are animal models relevant to key aspects of human parturition? Am J Physiol Regul Integr Comp Physiol 2009; 297: R525–R545.
15. Carter AM. Animal models of human placentation–a review. Placenta 2007; 28(Suppl A):S41–S47.
16. Valdes G, Erices R, Chacon C, Corthorn J. Angiogenic, hyperpermeability and vasodilator network in utero-placental units along pregnancy in the guinea-pig (Cavia porcellus). Reprod Biol Endocrinol 2008; 6:13.
17. Mess A, Zaki N, Kadyrov M, Korr H, Kaufmann P. Caviomorph placentation as a model for trophoblast invasion. Placenta 2007; 28: 1234–1238.
18. Castaneda-Gutierrez E, Pouteau E, Pescia G, Moulin J, Aprikian O, Mace K. The guinea pig as a model for metabolic programming of adiposity. Am J Clin Nutr 2011; 94:1838S–1845S.
19. Kaufmann P. Guinea pig Cavia porcellus. In: Benirschke K (ed.), Comparative Placentation. http://placentation.ucsd.edu/2004.
20. Moore LG, Charles SM, Julian CG. Humans at high altitude: hypoxia and fetal growth. Respir Physiol Neurobiol 2011; 178:181–190.
21. Al-Hasan YM, Pinkas GA, Thompson LP. Prenatal hypoxia reduces mitochondrial protein levels and cytochrome c oxidase activity in offspring guinea pig hearts. Reprod Sci 2014; 21:883–891.
22. Thompson LP, Dong Y. Chronic hypoxia decreases endothelial nitric oxide synthase protein expression in fetal guinea pig hearts. J Soc Gynecol Investig 2005; 12:388–395.
23. Oh C, Dong Y, Liu H, Thompson LP. Intrauterine hypoxia upregulates proinflammatory cytokines and matrix metalloproteinases in fetal guinea pig hearts. Am J Obstet Gynecol 2008; 199:78 e71–e76.
24. Chou SC, Azuma Y, Varia MA, Raleigh JA. Evidence that involucrin, a marker for differentiation, is oxygen regulated in human squamous cell carcinomas. Br J Cancer 2004; 90:728–735.
25. Schmittgen TD, Livak KJ. Analyzing real-time PCR data by the comparative CT method. Nature Protocols 2008; 3:1101–1108.
26. Davies J, Dempsey EW, Amoroso EC. The subplacenta of the guinea-pig: development, histology and histochemistry. J Anat 1961; 95:457–473.
27. Kaufmann P, Mayhew TM, Charnock-Jones DS. Aspects of human fetoplacental vasculogenesis and angiogenesis. II. Changes during normal pregnancy.Placenta 2004; 25:114–126.
28. Mess A. The subplacenta in Octodon degus and Petromus typicus–two hystricognath rodents without significant placental lobulation. J Exp Zool B Mol Dev Evol 2007; 308:172–188.
29. Huppertz B, Gauster M, Orendi K, Konig J, Moser GJ. Maternal uterine vascular remodeling during pregnancy. Anat 2009; 215:14–20.
30. Huppertz B. Oxygenation of the placenta and its role in pre-eclampsia. Pregnancy Hypertens 2014; 4:244–245.
31. Mateev S, Sillau AH, Mouser R, McCullough RE, White MM, Young DA, Moore LG. Chronic hypoxia opposes pregnancy-induced increase in uterine artery vasodilator response to flow. Am J Physiol Heart Circ Physiol 2003; 284:H820–H829.
32. Rockwell LC, Keyes LE, Moore LG. Chronic hypoxia diminishes pregnancy-associated DNA synthesis in guinea pig uteroplacental arteries. Placenta 2000; 21:313–319.
33. Burton GJ, Jauniaux E, Charnock-Jones DS. The influence of the intrauterine environment on human placental development. Int J Dev Biol 2010; 54:303–312.
34. Myatt L, Webster RP. Vascular biology of preeclampsia. J Thromb Haemost 2009; 7:375–384.
35. Osol G, Moore LG. Maternal uterine vascular remodeling during pregnancy. Microcirculation 2014; 21:38–47.
36. Bacon BJ, Gilbert RD, Kaufmann P, Smith AD, Trevino FT, Longo LD. Placental anatomy and diffusing capacity in guinea pigs following long-term maternal hypoxia. Placenta 1984; 5:475–487.
37. Matheson H, Veerbeek JH, Charnock-Jones DS, Burton GJ, Yung HW.

Morphological and molecular changes in the murine placenta exposed to normobaric hypoxia throughout pregnancy. J Physiol 2016; 594: 1371–1388.

38. Richter HG, Camm EJ, Modi BN, Naeem F, Cross CM, Cindrova-Davies T, Spasic-Boskovic O, Dunster C, Mudway IS, Kelly FJ, Burton GJ, Poston L, et al. Ascorbate prevents placental oxidative stress and enhances birth weight in hypoxic pregnancy in rats. J Physiol 2012; 590:1377–1387.

39. Kimball R, Wayment M, Merrill D, Wahlquist T, Reynolds PR, Arroyo JA. Hypoxia reduces placental mTOR activation in a hypoxia-induced model of intrauterine growth restriction (IUGR). Physiol Rep 2015; 3: e12651.

40. Cuffe JS, Walton SL, Singh RR, Spiers JG, Bielefeldt-Ohmann H, Wilkinson L, Little MH, Moritz KM. Mid- to late term hypoxia in the mouse alters placental morphology, glucocorticoid regulatory pathways and nutrient transporters in a sex-specific manner. J Physiol 2014; 592: 3127–3141.

41. Moore LG, Shriver M, Bemis L, Hickler B, Wilson M, Brutsaert T, Parra E, Vargas E. Maternal adaptation to high-altitude pregnancy: an experiment of nature–a review. Placenta 2004; 25(Suppl A):S60–S71.

42. Zamudio S. High-altitude hypoxia and preeclampsia. Front Biosci 2007; 12:2967–2977.

43. Keyes LE, Armaza JF, Niermeyer S, Vargas E, Young DA, Moore LG. Intrauterine growth restriction, preeclampsia, and intrauterine mortality at high altitude in Bolivia. Pediatr Res 2003; 54:20–25.

44. Zamudio S, Torricos T, Fik E, Oyala M, Echalar L, Pullockaran J, Tutino E, Martin B, Belliappa S, Balanza E, Illsley NP. Hypoglycemia and the origin of hypoxia-induced reduction in human fetal growth. PLoS One 2010; 5:e8551.

45. Lewis RM, Doherty CB, James LA, Burton GJ, Hales CN. Effects of maternal iron restriction on placental vascularization in the rat. Placenta 2001; 22:534–539.

46. Higgins JS, Vaughan OR, Fernandez de Liger E, Fowden AL, Sferruzzi-Perri AN. Placental phenotype and resource allocation to fetal growth are modified by the timing and degree of hypoxia during mouse pregnancy. J Physiol 2016; 594:1341–1356.

47. Gilbert RD, Cummings LA, Juchau MR, Longo LD. Placental diffusing capacity and fetal development in exercising or hypoxic guinea pigs. J Appl Physiol Respir Environ Exerc Physiol 1979; 46:828–834.

48. Steegers EA, von Dadelszen P, Duvekot JJ, Pijnenborg R. Pre-eclampsia. Lancet 2010; 376:631–644.

49. Huppertz B. Trophoblast differentiation, fetal growth restriction and preeclampsia. Pregnancy Hypertens 2011; 1:79–86.

50. Xie Y, Zhou S, Jiang Z, Dai J, Puscheck EE, Lee I, Parker G, Huttemann M, Rappolee DA. Hypoxic stress induces, but cannot sustain trophoblast stem cell differentiation to labyrinthine placenta due to mitochondrial insufficiency. Stem Cell Res 2014; 13:478–491.

51. Caniggia I, Winter J, Lye SJ, Post M. Oxygen and placental development during the first trimester: implications for the pathophysiology of pre-eclampsia. Placenta 2000; 21(Suppl A):S25–S30.

52. Rosario GX, Konno T, Soares MJ. Maternal hypoxia activates endovascular trophoblast cell invasion. Dev Biol 2008; 314:362–375.

53. Soares MJ, Chakraborty D, Kubota K, Renaud SJ, Rumi MA. Adaptive mechanisms controlling uterine spiral artery remodeling during the establishment of pregnancy. Int J Dev Biol 2014; 58:247–259.